

Distributed Data-Driven Predictive Control for Hybrid Connected Vehicle Platoons With Guaranteed Robustness and String Stability

Jingzheng Guo^{ID}, Hongyan Guo^{ID}, Member, IEEE, Jun Liu, Dongpu Cao^{ID}, Member, IEEE, and Hong Chen^{ID}, Senior Member, IEEE

Abstract—As a critical component of the Internet of Things, connected automated vehicles (CAVs) are progressively gaining attention for their benefits in terms of increased safety and reduced traffic congestion. In this article, a novel distributed data-driven model-predictive control (DDMPC) approach including feedforward for disturbance is proposed for cruise control of a hybrid platoon with a combination of human-operated and autonomous vehicles. By employing a predictor constructed from input/output data, predictive controllers are obtained without depending on the characteristic information of the system. A robustness analysis is performed with a combination of the input-to-state stability (ISS) theory with the sampled-data systems theory, and the L_2 -norm string stability is ensured by strict mathematical proof. In addition, we also discuss the asymptotic stability when the controller switches. CarSim simulation and bench experiment results verify that the DDMPC for connected vehicles can be robust to velocity disturbances and achieve satisfactory performance in ensuring string stability.

Index Terms—Distributed data-driven predictive control, hybrid connected vehicles, robustness, sampled system string stability.

I. INTRODUCTION

WITH the growth of communication technology, the Internet of Everything is progressively becoming a reality. Among the systems in this technology, intelligent transportation systems (ITSs) are a critical component of the Internet of Things, which will improve the convenience and efficiency of human existence. As a significant mode of transportation, connected automated vehicles (CAVs) benefit from

Manuscript received 28 November 2021; revised 11 January 2022; accepted 7 February 2022. Date of publication 17 February 2022; date of current version 24 August 2022. This work was supported in part by the National Natural Science Foundation of China under Grant U19A2069, Grant 61790563, and Grant U1964202; and in part by the Project of Science and Technology, Department of Jilin Province under Grant 20200401088GX. (Corresponding author: Hongyan Guo.)

Jingzheng Guo, Hongyan Guo, and Jun Liu are with the State Key Laboratory of Automotive Simulation and Control and the Department of Control Science and Engineering, Jilin University (Campus Nanling), Changchun 130025, China (e-mail: gojzheng@126.com; guohy11@jlu.edu.cn; liujun20@jlu.edu.cn).

Dongpu Cao is with the Department of Mechanical and Mechatronics Engineering, University of Waterloo, Waterloo, ON N2L 3G1, Canada (e-mail: dongpu.cao@uwaterloo.ca).

Hong Chen is with the Clean Energy Automotive Engineering Center, Tongji University, Shanghai 201804, China, and also with the Department of Control Science and Engineering, Jilin University, Changchun 130012, China (e-mail: chenh@jlu.edu.cn).

Digital Object Identifier 10.1109/JIOT.2022.3152165

the advantages of these systems in terms of safety and congestion reduction, particularly on highways, and have garnered considerable attention from many research institutions [1], [2]. Among the numerous platoon studies, cooperative control of the platoon is the focus of current research [3], [4].

To minimize vehicle collisions and increase traffic performance, adaptive cruise control (ACC) was developed. The system senses the distance between two adjacent vehicles using light detection and ranging (LiDAR) and other devices, and the controller adjusts the speed to preserve a set distance between the vehicles [5]. Although the ACC framework can ensure the platoon's safety, the control stability cannot be guaranteed. By taking advantage of the rapid growth of wireless networking, especially the dense deployment of the fifth-generation (5G) terrestrial network, information can be transmitted in real time on vehicle-to-all (V2X) products, such as vehicle-to-vehicle (V2V) and vehicle-to-Internet (V2I) services [6], [7]. Improvements to the cooperative ACC (CACC) system are discussed in [8] and [9]. Benefiting from the application of the communication topology, CACC has satisfactory performance in string instability [10] and better resolves the situation of traffic congestion [11]. However, the penetration rate of automated driving control cars is still limited, which makes it challenging to control vehicles in accordance with the CACC model. Zhu and Zhang [12] carried out research on vehicles in a hybrid connected vehicle platoon containing n human-driven vehicles and an autonomous vehicle, which is more compatible with existing patterns in traffic. Thus, the problem of hybrid platoons has attracted increasing research effort.

For the control of cooperative systems, model-based control methods are often used to control autonomous vehicles in [13] and [14]. After making full use of the information given by the model, the controller can achieve the optimal or sub-optimal control effect for the controlled object. However, the performance of a model-based control system is dependent on the accuracy of the model [15]. Therefore, based on the above considerations, data-driven or model-free optimal control is urgently needed. For complex systems such as vehicles, the advantages of data-driven control methods are more obvious. For the cruise system, Zhao *et al.* [16] applied data-driven optimal control to intelligent cruise control. Zhu *et al.* [17] applied data-driven adaptive dynamic programming (ADP) to heterogeneous CACC system control. Guo *et al.* [18] used

the model-free adaptive three-step method for truck platoon cruise control. Gao *et al.* [19] applied the ADP control method for the control of a connected cruise control (CCC) system. However, for the existing data-driven methods, neural networks or other methods are often used to approximate the optimal solution in the form of iteration, which places higher requirements on the collected data; in addition, the iterative process tends to increase the computational burden. These factors limit the practical implementation of data-driven methods.

To resolve the problems mentioned above, by combining the advantages of data identification and predictive control, we propose a data-driven predictive control method that eliminates the requirements of the system state-space equation or transfer function, and its ability to solve the optimal problem in the rolling time domain through optimization endows it with the inherent characteristics to compensate for communication delays [20]–[22]. The algorithm constructs a linear predictor based on the data sets to characterize the system's behavior, thus minimizing system errors induced by model mismatch. Compared with data-driven ADP, this method does not need to solve a nonlinear algebraic Riccati equation (ARE), and in the case of generalized predictive control (GPC), it also avoids solving a recursive Diophantine equation [23]. The proposed approach, in contrast to the data-driven control method based on neural networks, does not require a large number of basic functions, decreases computational burden, and hence reduces hardware requirements in applications. Furthermore, the data processing mechanism of data-driven predictive control is based on singular value decomposition (SVD) and the projection method, enabling an approach with the advantage of numerical stability [24].

Therefore, the motivation for employing data-driven model predictive control (MPC) can be summarized as follows: first, an interconnected system with a dynamic unknown, data-driven MPC reconstructed system through a data set can more accurately reflect system characteristics than a mechanism-based model. Second, the numerical stability and lower computational complexity of the data-driven MPC provide it with better online application prospects.

For interconnected systems, asymptotic stability is a critical criterion for evaluating the performance of controller design. Swaroop and Hedrick [25] and Ma *et al.* [26], describing the core characteristics of the connected vehicles, indicate that the fluctuation of the disturbance reduces (e.g., speed deviation) or remains constant as it propagates along the vehicle platoon. A significant number of analyses on string stability research have been carried out [27], [28]. In addition, in [29], the researchers investigated the frequency domain string stability characteristics of platoons, which ignores the impact of external disturbance. According to the \mathcal{L}_p -norm employed to characterize the perturbation amplitude, a novel string stability definition was proposed in [30], which is based on the notion of \mathcal{L}_p stability. This new concept not only accommodates initial condition perturbations and external disturbances but also applies to linear and nonlinear systems. Therefore, we introduce \mathcal{L}_p string stability into the hybrid platoon control system.

Reviewing the above literature, we can see that the existing multivehicle system research focuses mainly on platoon control composed of autonomous vehicles, while hybrid platoons composed of human-driven and autonomous vehicles are more in line with the current traffic scene. Taking into account the dynamic uncertainty in the hybrid system and the influence of communication on the system, we propose a data-driven MPC strategy that combines subspace prediction and predictive control to address dynamic disturbances and improve system performance. We focus on theoretically analyzing the robustness and string stability of the system considering data sampling. The main contributions of this study are as follows.

- 1) For hybrid platoons with unknown dynamics, we propose a distributed data-driven predictive control (DDMPC) scheme including feedforward compensation. Unlike the existing model prediction method (MPC) of designing a controller through a mechanism model [22], this scheme uses only the actual and recent historical data of the system to generate correct control behavior while also suppressing measurable speed disturbances. In this strategy, the subspace predictor is constructed by SVD and the projection method, and the system parameters can be obtained in a single calculation, which is different from the existing data-driven methods of employing neural networks and iterating to approximate the system model [16]–[19], so the scheme potentially reduces the complexity.
- 2) We provide a robustness analysis of interconnected systems through the comprehensive combination of input-to-output stability (IOS) theory and sampled-data systems theory. Different from the existing robustness analysis only for discrete-time or continuous-time systems [31], [32], the system stability research of data-driven MPC based on the sampling theory solves the robustness analysis problem of hybrid dynamic systems, which are composed of continuous-time and discrete-time systems. Advantages over the existing method mentioned above lie in that we provide the upper bound of the difference between the state of the system at the sampling moment and the state of the continuous system while selecting the sampling interval reasonably.
- 3) We analyze and prove the \mathcal{L}_2 string stability of autonomous vehicles in hybrid platoons in the face of external disturbance. In contrast to the existing Lyapunov-based, finite-length strings and frequency-domain string stability analysis [27]–[29], \mathcal{L}_2 string stability not only considers the velocity variations of the leading vehicle and the nonzero initial conditions but also relaxes the requirements for the length of the platoon. Simulations in CarSim and bench experiments verify the theoretical analysis and the feasibility of the proposed method.

The remainder of this article is arranged as follows: Section II deduces the mathematical model of the hybrid vehicle platoon. Section III details the proposed distributed data-driven predictive control approach considering disturbance. In Section IV, mathematical proofs of the IOS and

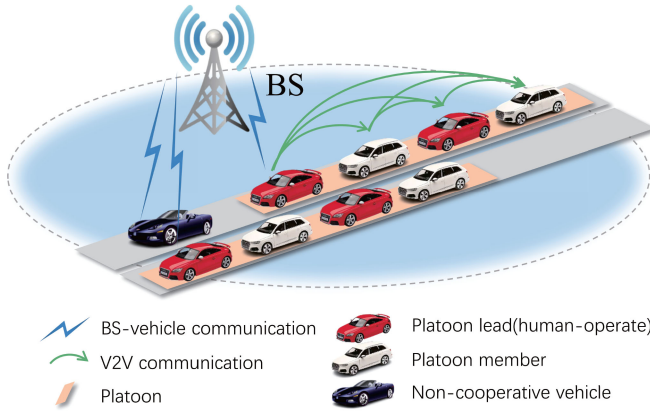


Fig. 1. Schematic of hybrid platoon scenario under V2X communication, where BS-vehicle communication refers to the communication between the base station and the leading vehicle in the platoon, and the noncooperative vehicle is independent of platoons. The white cars in the platoon are autonomous vehicles, and the red cars are human-driven vehicles.

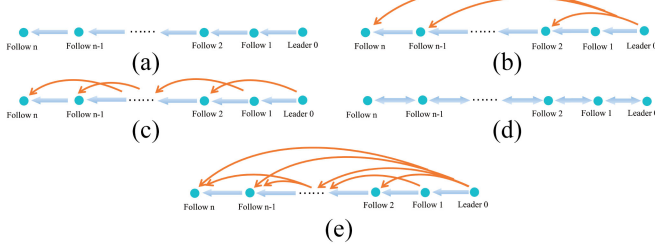


Fig. 2. Typical IFTs for CAV Platoon. (a) PF. (b) PFL. (c) BDL. (d) BD. (e) TPLF.

\mathcal{L}_2 -norm string stability are given. Sections V and VI present the results of simulations and experiments, respectively. The final section discusses conclusions and possible future study.

Notations: In this article, $|\cdot|$ stands for the norm of vectors and matrices. $\lambda_{\max}(Q)$ and $\lambda_{\min}(Q)$ represent the max/min eigenvalues of a real symmetric matrix Q , respectively. In addition, the continuous α is of class \mathcal{K} if it is strictly increasing and satisfies $\alpha(0) = 0$. A continuous function β belongs to class \mathcal{KL} when the following two conditions are met: for fixed variables a , the function $\beta(\cdot, a)$ is of class \mathcal{K} and, for each fixed variable b , the function $\beta(b, \cdot)$ is decreasing and converges to 0 at infinity.

II. MATHEMATICAL MODELING

For a hybrid connected vehicle platoon composed of human-driven and autonomous vehicles, as shown in Fig. 1, the speed and position signals are exchanged between vehicles through V2V communication. Several common information flow topologies (IFTs) at present are shown in Fig. 2. Rapid changes in the wireless network topology and frequent communication link switching will cause the V2X network to appear unstable and introduce network data packet loss. Platoon control performance, especially system stability, is deeply affected by packet loss [33]. To minimize the impact on the stability of the multivehicle system caused by packet loss, we adopt a fixed communication topology in this article. Here, we choose the two-predecessor-leader-following (TPLF)

communication mode. Through wireless communication technology, each autonomous vehicle can receive the information of the two preceding vehicles and the leading vehicle.

We consider a platoon with $n+1$ (n is odd) vehicles traveling in a straight path in this study in which the behaviors of the i th human-driven vehicle can be described as

$$\begin{aligned}\dot{h}_i &= v_{i-1} - v_i \\ \dot{v}_i &= \alpha_i(V(h_i) - v_i) + \beta_i \dot{h}_i\end{aligned}\quad (1)$$

where $i = 3, 5, 7, \dots, n$; h_i represents the distance between two vehicles i and $i-1$, and the speed of vehicle i is v_i . Variables α_i and β_i are human parameters related to driving behavior, representing headway gain and relative speed gain, respectively, and satisfying $\alpha_i > 0$, $\alpha_i + \beta_i > 0$. $V(\cdot)$ denotes a range strategy

$$V(h) = v_{\max} \begin{cases} 0, & h \in [0, l] \\ \frac{((h-h_{\text{stop}})/s)^3}{1+((h-h_{\text{stop}})/s)^3}, & h \in [l, \infty]. \end{cases} \quad (2)$$

The strategy indicates that vehicle i remains stationary if $h_i \leq l$, which means that drivers tend to stop in heavy traffic. Here, v_i increases with increasing h_i if $h_i \geq l$. Additionally, when the spacing h_i is very large, vehicle i aims to drive at a maximum speed of v_m , which means that in very sparse scenarios, the driver's objective is to travel at the maximum possible speed, usually referred to as free flow. Based on the self-regulating mechanisms, the driver aims to achieve the desired speed $v^* = V(h^*)$ while obtaining the desired spacing h^* . The parameters α_i and β_i vary for drivers with different driving styles.

We define distance error $\Delta h_i = h_i - h^*$ and velocity error $\Delta v_i = v_i - v^*$. In the desired equilibrium state (h^*, v^*) , we linearize the nonlinear model (1) by using the Taylor method

$$\begin{aligned}\dot{\Delta h}_i &= \Delta v_{i-1} - \Delta v_i \\ \dot{\Delta v}_i &= \frac{\alpha_i}{\tau_f} \Delta h_i - (\alpha_i + \beta_i) \Delta v_i + \beta_i \Delta v_{i-1}\end{aligned}\quad (3)$$

where $\tau_f = 1/V'(h^*)$ represents the time headway, with $V'(h^*)$ being the derivative of the strategy $V(h)$.

The intelligent CAV following human-driven vehicles that receives information through a communication device can be described as follows:

$$\begin{aligned}\dot{\Delta h}_{i+1} &= \Delta v_i - \Delta v_{i+1} \\ \dot{\Delta v}_{i+1} &= u_{i+1}\end{aligned}\quad (4)$$

where u_{i+1} denotes the control input. In this article, this parameter represents the acceleration of the vehicle.

The communication delay in V2X is known to affect the response characteristics of the system and even cause system instability [34]. To guarantee the dynamic properties of the system in the presence of communication delay, the constant time headway (CTH) spacing policy, which is the basis of the fault-tolerant strategy, is adopted for CAVs to improve the string stability [35] and safety. The desired distance $h_{i+1,des}^*$ between two neighboring vehicles is expressed as $h_{i+1,des}^* = \tau_{i+1} v_{i+1} + \tilde{h}_{i+1}$, where τ_{i+1} refers to the nominal headway, and \tilde{h}_{i+1} is the desired standstill distance. Therefore,

for autonomous vehicles, the distance error is defined as $\Delta h_{i+1} = h_{i+1} - \tau_{i+1} v_{i+1} - \tilde{h}_{i+1}$.

Then, the error dynamics for autonomous vehicles are described by

$$\begin{bmatrix} \Delta \dot{h}_{i+1} \\ \Delta \dot{v}_{i+1} \end{bmatrix} = N_i \begin{bmatrix} \Delta h_{i+1} \\ \Delta v_{i+1} \end{bmatrix} + M_i \begin{bmatrix} \Delta h_i \\ \Delta v_i \end{bmatrix} + B_i u_{i+1} \quad (5)$$

where

$$N_i = \begin{bmatrix} 0 & -1 \\ 0 & 0 \end{bmatrix}, M_i = \begin{bmatrix} 0 & 1 \\ 0 & 0 \end{bmatrix}, B_i = \begin{bmatrix} -\tau_{i+1} \\ 1 \end{bmatrix}.$$

Combining (3) and (5), we obtain the hybrid platoon model interconnected by the i th human-driven and the $i+1$ th autonomous vehicles under the TPLF topology

$$\dot{x} = Ax + Bu + K\Delta v_{i-1} \quad (6)$$

where $x = [\Delta h_i, \Delta v_i, \Delta h_{i+1}, \Delta v_{i+1}]^T$, $u = u_{i+1} \in \mathbb{R}^1$, and Δv_{i-1} is a bounded disturbance. In (6), $A \in \mathbb{R}^{4 \times 4}$, $B \in \mathbb{R}^{4 \times 1}$, and $K \in \mathbb{R}^{4 \times 1}$ are given as follows:

$$\begin{aligned} A &= \begin{bmatrix} F_i & 0 \\ M_i & N_i \end{bmatrix}, B = \begin{bmatrix} 0_{2 \times 1} \\ B_i \end{bmatrix} \\ K &= \begin{bmatrix} [1 & \beta_i] & 0_{1 \times 2} \end{bmatrix}^T \end{aligned}$$

where

$$F_i = \begin{bmatrix} 0 & -1 \\ \frac{\alpha_j}{\tau_f} & -\alpha_i - \beta_i \end{bmatrix}.$$

For the vehicles in the TPLF topology, the state information of the $i+1$ th autonomous vehicle and the previous i th human-driven vehicle is available, resulting in the output equation

$$y = Cx \quad (7)$$

where C is an identity matrix and $y \in \mathbb{R}^{4 \times 1}$ is the output of the system states.

III. DISTRIBUTED DATA-DRIVEN PREDICTIVE CONTROL

The cost requirements for connected vehicles are derived in this section based on the following considerations.

- 1) Taking traffic safety and throughput into consideration, the V2V distance should not be too short or too long.
- 2) For scheduling reasons, the target velocity of each vehicle should be near the desired velocity v^* , which means that Δv_i should be as minimal as possible.
- 3) Maintaining driver comfort necessitates that the vehicle accelerates smoothly.

To meet the above-mentioned control criteria and considering the application based on the communication scheme and the excellent performance of the distributed method in platoon control [36]–[38], we designed a distributed data-driven predictive controller in this section. The controller is composed of two parts, namely, the subspace predictor and the predictive controller. The subspace predictor is constructed by the input and output information directly to forecast the dynamic output of the plant without an explicit model. The design of the predictive controller is derived from the predictive control theory.

A. Design of Subspace Predictor

The state-space model is chosen as the model from which to derive the subspace predictor. If the process disturbances are measurable, e.g., the speed variation of the leading car, because we know that measurable disturbance is an input variable to the process and cannot be manipulated to affect the process output, then the discrete-time form of the state-space expression with disturbances for the linear system is represented by the following:

$$x_{k+1} = \tilde{A}x_k + \tilde{B}u_k + \tilde{K}\Delta v_{i-1} \quad (8a)$$

$$y_k = \tilde{C}x_k. \quad (8b)$$

For the connected vehicles, Δv_1 is the measurable disturbance variable, and acceleration a is determined to be the control input, so u_k can be expressed here as $u_k = a$.

The control output $y(k) \in \mathbb{R}$ is made up of the distance and velocity errors discussed in Section II. Therefore, $y(k)$ can be written as $y_k = [\Delta h_i(k), \Delta v_i(k), \Delta h_{i+1}(k), \Delta v_{i+1}(k)]^T$.

In the state-space expression, $x(k) \in \mathbb{R}^n$ (n is the order of the state) is the state of the system, with coefficient matrices A, B, K , and C describing the dynamic characteristics of the connected vehicles. For a system with q -input and o -output, A, B , and C are $(n \times n)$, $(n \times q)$, and $(o \times n)$ matrices, respectively.

As the data-driven part of DDMPC, the subspace predictor utilizes the data set to construct a system model with dynamic uncertainty to predict the future state of the system.

Through the open-loop system experiment, the measurement data of the input $u(k)$, the disturbance $\Delta v(k)$ and the output $y(k)$ are collected. These data are divided into two parts: 1) the history and 2) the future, to construct the Hankel matrix, which is an important part of the subspace predictor. The data-based Hankel matrices $U_p, U_f, \Delta V_p, \Delta V_f, Y_p$, and Y_f constructed by collected data are shown in Table I, where the historical and future observable data sets are represented by p and f , respectively. Each Hankel matrix is made up of rows of i blocks and columns of j blocks. The blocks are vectors of data, i.e., $y_i = [y_{i1}, y_{i2}, \dots, y_{il}]^T$. The sequence of past and future states is expressed as

$$\begin{aligned} X_p &= [x_0 \quad x_1 \quad \dots \quad x_{j-1}] \\ X_f &= [x_i \quad x_{i+1} \quad \dots \quad x_{i+j-1}]. \end{aligned}$$

By recursively substituting (8), the matrix expression of the output required for subspace system identification can be expressed as

$$Y_f = \Gamma_i X_f + H_i U_f + H_i^v \Delta V_f. \quad (9)$$

The output Y_f can be predicted using the following prediction expressions:

$$\hat{Y}_f = L_w W_p + L_u U_f + L_v \Delta V_f \quad (10)$$

where $W_p = [Y_p \quad U_p \quad \Delta V_p]^T$, the observability matrix $\Gamma_i(im \times n)$ and the lower triangular Toeplitz matrices $H_i(im \times il)$ are as follows:

$$\Gamma_i = \begin{bmatrix} \tilde{C} \\ \tilde{C}\tilde{A} \\ \vdots \\ \tilde{C}\tilde{A}^{i-1} \end{bmatrix}, H_i = \begin{bmatrix} 0 & 0 & \dots & 0 \\ \tilde{C}\tilde{B} & 0 & \dots & 0 \\ \dots & \dots & \dots & \dots \\ \tilde{C}\tilde{A}^{i-2}\tilde{B} & \tilde{C}\tilde{A}^{i-3}\tilde{B} & \dots & 0 \end{bmatrix}$$

TABLE I
HANKEL MATRIX RECONSTRUCTED FROM OBSERVABLE DATA BLOCKS

Type	Reconstruction matrix	Type	Reconstruction matrix	Type	Reconstruction matrix
U_p	$\begin{bmatrix} u_0 & u_1 & \cdots & u_{j-1} \\ u_1 & u_2 & \cdots & u_j \\ \vdots & \vdots & \cdots & \vdots \\ u_{i-1} & u_i & \cdots & u_{i+j-2} \end{bmatrix}$	Y_p	$\begin{bmatrix} y_0 & y_1 & \cdots & y_{j-1} \\ y_1 & y_2 & \cdots & y_j \\ \vdots & \vdots & \cdots & \vdots \\ y_{i-1} & y_i & \cdots & y_{i+j-2} \end{bmatrix}$	ΔV_p	$\begin{bmatrix} \Delta v_0 & \Delta v_1 & \cdots & \Delta v_{j-1} \\ \Delta v_1 & \Delta v_2 & \cdots & \Delta v_j \\ \vdots & \vdots & \cdots & \vdots \\ \Delta v_{i-1} & \Delta v_i & \cdots & \Delta v_{i+j-2} \end{bmatrix}$
U_f	$\begin{bmatrix} u_i & u_{i+1} & \cdots & u_{i+j-1} \\ u_{i+1} & u_{i+2} & \cdots & u_{i+j} \\ \vdots & \vdots & \cdots & \vdots \\ u_{2i-1} & u_{2i} & \cdots & u_{2i+j-2} \end{bmatrix}$	Y_f	$\begin{bmatrix} y_i & y_{i+1} & \cdots & y_{i+j-1} \\ y_{i+1} & y_{i+2} & \cdots & y_{i+j} \\ \vdots & \vdots & \cdots & \vdots \\ y_{2i-1} & y_{2i} & \cdots & y_{2i+j-2} \end{bmatrix}$	ΔV_f	$\begin{bmatrix} \Delta v_i & \Delta v_{i+1} & \cdots & \Delta v_{i+j-1} \\ \Delta v_{i+1} & \Delta v_{i+2} & \cdots & \Delta v_{i+j} \\ \vdots & \vdots & \cdots & \vdots \\ \Delta v_{2i-1} & \Delta v_{2i} & \cdots & \Delta v_{2i+j-2} \end{bmatrix}$

$$H_i^v = \begin{bmatrix} 0 & 0 & \cdots & 0 \\ \tilde{C}\tilde{K} & 0 & \cdots & 0 \\ \vdots & \cdots & \cdots & \cdots \\ \tilde{C}\tilde{A}^{i-2}\tilde{K} & \tilde{C}\tilde{A}^{i-3}\tilde{K} & \cdots & 0 \end{bmatrix}. \quad (11)$$

The subspace matrices L_w , L_u , and L_v are generated by employing the least squares approach to solve the extreme value issue and predict the future output Y_f

$$\min_{L_w, L_u, L_v} \left| Y_f - (L_w \quad L_u \quad L_v) \begin{pmatrix} W_p \\ U_f \\ \Delta V_f \end{pmatrix} \right|_F^2 \quad (12)$$

$$\hat{Y}_f = Y_f / \begin{bmatrix} W_p \\ U_f \\ \Delta V_f \end{bmatrix}. \quad (13)$$

\hat{Y}_f is obtained by projecting the space of Y_f to the subspace defined by W_p , U_f , and ΔV_f . Therefore, the matrices L_w , L_u , and L_v is calculated as follows:

$$\begin{bmatrix} L_w & L_u & L_v \end{bmatrix} = Y_f \begin{bmatrix} W_p^T & U_f^T & \Delta V_f^T \end{bmatrix} \left(\begin{bmatrix} W_p \\ U_f \\ \Delta V_f \end{bmatrix} \begin{bmatrix} W_p^T & U_f^T & \Delta V_f^T \end{bmatrix} \right)^{-1}. \quad (14)$$

B. Predictive Controller Design

The control requirement for autonomous vehicles is to track the desired speed v^* and spacing h^* , i.e., to make the actual velocity v converge to the specified reference sequence $R_f(k+1)$. Furthermore, after completing the design of the predictor according to the predictive control theory [22] and the subspace identification method, at time k , the velocity error Δv_i and distance error Δh_i can be predicted. The prediction horizon is represented in this article using N_p , and the control horizon is N_u , satisfying $N_p \geq N_u$. We define reference sequences as follows:

$$R_f(k+1) = [r_f(k+1) \quad r_f(k+2) \quad \cdots \quad r_f(k+N_p)]^T.$$

For the connected vehicles, the sequences of control inputs $u_f(k)$ and predictive control outputs $\hat{y}_f(k+1)$ can be summed

up as

$$\hat{y}_f(k+1) = \begin{bmatrix} \hat{y}(k+1) \\ \hat{y}(k+2) \\ \vdots \\ \hat{y}(k+N_p) \end{bmatrix}, u_f(k) = \begin{bmatrix} u(k) \\ u(k+1) \\ \vdots \\ u(k+N_u-1) \end{bmatrix}.$$

Typically, to minimize the difference between the reference and predicted output, we choose the quadratic form as the cost criterion, and control inputs u may also be incorporated as a penalty for control characteristics. Therefore, the description of the cooperative control optimization issue is as follows:

$$\min_{u_f(k)} J(\hat{y}(k), u_f(k), N_p, N_u) \quad (15a)$$

$$J = \|\Gamma_y(\hat{y}_f(k+1) - R_f(k+1))\|^2 + \|\Gamma_u u_f(k)\|^2 \quad (15b)$$

where the matrices $\Gamma_y = \text{diag}(\gamma_{y,1}, \gamma_{y,2}, \dots, \gamma_{y,N_p})$ and $\Gamma_u = \text{diag}(\gamma_{u,1}, \gamma_{u,2}, \dots, \gamma_{u,N_u})$.

With the output sequence obtained by (10), the performance criterion J can be written as

$$J = (L_w w_p + L_u u_f + L_v \Delta v_f - r_f)^T \Gamma_y (L_w w_p + L_u u_f + L_v \Delta v_f - r_f) + u_f^T \Gamma_u u_f. \quad (16)$$

Setting the trace of the derivative of J with respect to the input sequence u_f to 0, we have: $\partial J / \partial u_f = 0$.

Then, the control law with feedforward behavior becomes

$$u_f = (\Gamma_u + L_u^T \Gamma_y L_u)^{-1} L_u^T \Gamma_y (r_f - L_w w_p - L_v \Delta v_f). \quad (17)$$

Only the first element u_1 is implemented

$$u_1 = -L_w^f w_p - L_v^f \Delta v_f + L_r^f r_f \quad (18)$$

where L_r^f , L_w^f , and L_v^f are defined as

$$\begin{aligned} L_r^f &= \left\{ (\Gamma_u + L_u^T \Gamma_y L_u)^{-1} \right\} (1:m,:) L_u^T \Gamma_y \\ L_w^f &= L_r^f L_w \\ L_v^f &= L_r^f L_v. \end{aligned}$$

The DDMPC Algorithm 1 is given and the operation of Algorithm 1 is shown in Fig. 3.

We recombine the new vector $L_p = (L_w, L_v)$ in L_w and L_v , and then SVD is used to approximate L_p by a rank deficient matrix

$$L_p = (U_a \quad U_b) \begin{pmatrix} S_a & 0 \\ 0 & S_b \end{pmatrix} \begin{pmatrix} V_a^T \\ V_b^T \end{pmatrix} \approx U_a S_a V_a^T. \quad (19)$$

Algorithm 1 Data-Driven Predictive Control Algorithm

- 1: Construct the Hankel matrices Y_f , U_f , V_f , and W_p given in Table I using the measured input and output data;
- 2: Solve the following least squares problem for the unknown parameters L_w , L_u and L_v :
$$\min_{L_w, L_u, L_v} \left| Y_f - (L_w \ L_u \ L_v) \begin{pmatrix} W_p \\ U_f \\ \Delta V_f \end{pmatrix} \right|_F^2$$
- 3: Approximate $L_p = (L_w, L_v)$ by a rank-n matrix by taking the SVD, i.e.,

$$L_p = U_a S_a V_a^T$$
- 4: Reconstruct the data matrix as input:

$$W_p = [Y_p \ U_p \ \Delta V_p]^T$$
- 5: Calculate the control sequence u_f and apply the first element u_1 to the system:

$$u_f = (\lambda I + L_u^T L_u)^{-1} L_u^T (r_f - L_w w_p - L_v v_f)$$
- 6: To execute the subsequent control procedure, Step 4 needs to be repeated to construct a new W_p^T composed of the latest measurement output y , control law u and measurable interference Δv_1 .

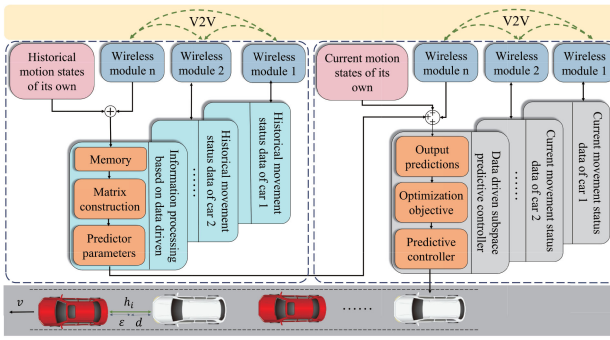


Fig. 3. Overview of the DDMPC architecture with the hybrid connected vehicle system.

For mathematical models established in Section II, the reference trajectory has been included in the state vector, so the value of the reference r_f in the control law can be seen as zero, and we rewrite the control law in the general form of state feedback

$$u_1 = -L_r^f U_a S_a^{1/2} x. \quad (20)$$

IV. ROBUSTNESS AND STRING STABILITY

In this section, we let $k_d = L_r^f U_a S_a^{1/2}$ and the control policy becomes as follows:

$$u_k = -k_d x_k \quad (21)$$

where x_k is the state at sampling time $t = dT$.

Then, we demonstrate the robust and asymptotic stabilization of system (6) using the above control policy when the time t is in the sampling interval $[dT, (d+1)T]$.

A. Robustness Analysis

Considering the control law (21) in the closed-loop system (6), we can obtain that

$$\dot{x} = (A - Bk_d)x + B[k_d(x - x_k)] + E\Delta v_{i-1}. \quad (22)$$

To perform robustness analysis, first, Lemma 1 is given, which determines the upper bound of the difference between the state of the system at the sampling moment and the state of the continuous system.

Lemma 1: Let $t \in [dT, (d+1)T]$. For any $\varepsilon_1, \varepsilon_2 > 0$, there exists an $\alpha > 0$ such that

$$\|k_d(x_t - x_k)\| \leq \varepsilon_1 |x_t| + \varepsilon_2 \|\Delta v_{i-1}\| \quad (23)$$

where

$$\varepsilon_1 = \frac{|k_d| \cdot \left| \int_0^{t-kT} e^{A\tau} d\tau \right| |A + Bk_d|}{|\alpha|}$$

$$\varepsilon_2 = \left| \int_0^{t-kT} e^{A\tau} d\tau \right| \cdot |E|.$$

Proof: Denote $x(t)$ by x_t for simplicity. By (22), we have

$$x_t = e^{(t-kT)A} x_k + \int_{kT}^t e^{(t-\tau)A} d\tau (-Bk_d x_k + E\Delta v_{i-1}). \quad (24)$$

Then, we can derive

$$x_t - x_k = \int_0^{t-kT} e^{A\tau} d\tau \cdot (A + Bk_d)x_k - \int_0^{t-kT} e^{A\tau} d\tau \cdot E\Delta v_{i-1}. \quad (25)$$

There exists a parameter $\alpha > 0$ that satisfies $\alpha \cdot |x_k| \leq |x_t|$. Therefore, we can obtain that

$$|k_d(x_t - x_k)| \leq |k_d| \cdot |x_t - x_k|$$

$$\leq \frac{|k_d| \cdot \left| \int_0^{t-kT} e^{A\tau} d\tau \right| |A + Bk_d|}{|\alpha|} \cdot |\alpha| \cdot |x_k|$$

$$+ \left| \int_0^{t-kT} e^{A\tau} d\tau \right| \cdot |E| \|\Delta v_{i-1}\|$$

$$:= \varepsilon_1 |x_t| + \varepsilon_2 \|\Delta v_{i-1}\| \quad (26)$$

then (23) holds. ■

Theorem 1: Under the condition of Assumption 1, if ω_1 and ε_1 satisfy $\psi_1(\omega_1, \varepsilon_1) > 0$, system (6) with the controller (21) is an IOS system.

Proof: Choose an ISS-Lyapunov function $V = x^T P_d x$, where P_d is not only a positive definite symmetric matrix but also the solution to the Lyapunov equation below with $\omega > 0$

$$(A - BK)^T P_d + P_d (A - BK) = -\omega Q. \quad (27)$$

By [39], we can obtain $P_d = w \int_0^\infty e^{(A-BK)^T t} e^{(A-BK)t} dt$. Since $|e^{(A-BK)t}| \leq ce^{-\mu t}$, we have

$$|P_d| \leq \omega c^2 / 2\mu. \quad (28)$$

The derivative of the Lyapunov equation V at $dT \leq t \leq (d+1)T$ along the trajectory of system (22) is

$$\begin{aligned} \dot{V} &= \dot{x}^T P_d x + x^T P_d \dot{x} \\ &= x^T [(A - Bk_d)^T P_d + P_d (A - Bk_d)] x \\ &\quad + [B \cdot k_d (x - x_k)]^T P_d x + x^T P_d [B \cdot k_d \cdot (x - x_k)] \\ &\quad + (E\Delta v_{i-1})^T P_d x + x^T P_d \cdot E\Delta v_{i-1} \\ &= -\omega x^T Q x + 2x^T P_d B k_d (x - x_k) + 2x^T P_d E \Delta v_{i-1} \\ &\leq -\omega_1 |x|^2 + \varepsilon_1 |P_d| \|B\| \cdot |x|^2 + 2(\varepsilon_2 |P_d| \|B\|) \end{aligned}$$

$$\begin{aligned}
& + |P_d||E||x||\Delta v_{i-1}| \\
& \leq - \left(\omega_1 + \frac{\omega c^2}{2\mu} B_M \varepsilon_1 + \frac{\omega^2 c^4 (B_M^2 + E_M)}{4\mu^2} \right) |x|^2 \\
& + (\varepsilon_2^2 + 1) |\Delta v_{i-1}|^2 \\
& := -\psi_1 |x|^2 + \psi_2 |\Delta v_{i-1}|^2
\end{aligned} \tag{29}$$

where

$$\begin{aligned}
\psi_1 &= \omega_1 - \frac{\omega c^2}{2\mu} B_M \varepsilon_1 - \frac{\omega^2 c^4 (B_M^2 + E_M)}{4\mu^2} \\
\psi_2 &= \varepsilon_2^2 + 1.
\end{aligned} \tag{30}$$

We select ω_1 and ε_1 such that $\psi_1 > 0$. Then, according to the following inequality $\lambda_{\min}(P_d)|x|^2 \leq V \leq \lambda_{\max}(P_d)|x|^2$, it can be directly inferred from (22) that:

$$\begin{aligned}
V(t) &\leq \exp\left(-\frac{\psi_1}{\lambda_m} t\right) V(0) + \int_0^t \exp\left(-\frac{\psi_1}{\lambda_m} t\right) \cdot \psi_2 |\Delta v_{i-1}|^2 dt \\
&\leq \exp\left(-\frac{\psi_1}{\lambda_m} t\right) V(0) + \frac{\psi_2 \lambda_m}{\psi_1} \|\Delta v_{i-1}\|^2.
\end{aligned} \tag{31}$$

According to the comparison principle, an immediate consequence of the previous inequality is

$$\begin{aligned}
|x| &\leq \left(\frac{\exp\left(-\frac{\psi_1}{\lambda_m} t\right) V(0) + \frac{\psi_2 \lambda_m}{\psi_1} \|\Delta v_{i-1}\|^2}{\lambda_m} \right)^{1/2} \\
&\leq \left(\frac{\exp\left(-\frac{\psi_1}{\lambda_m} t\right) \cdot \lambda_M |x(0)|^2 + \frac{\psi_2 \lambda_m}{\psi_1} \|\Delta v_{i-1}\|^2}{\lambda_m} \right)^{1/2} \\
&= \exp\left(\frac{-\psi_1}{2\lambda_m} t\right) \sqrt{\frac{\lambda_M}{\lambda_m}} |x(0)| + \sqrt{\frac{\psi_2}{\psi_1}} \|\Delta v_{i-1}\| \\
&:= \sigma_x(|x(0)|, t) + \gamma_x(\|\Delta v_{i-1}\|)
\end{aligned} \tag{32}$$

where $\sigma_x(|x(0)|, t) = \exp\left(-\psi_1/2\lambda_m\right)t\sqrt{(\lambda_M/\lambda_m)}|x(0)|$ belongs to class \mathcal{KL} and $\gamma_x(\|\Delta v_{i-1}\|) = \sqrt{(\psi_2/\psi_1)}\|\Delta v_{i-1}\|$ is class \mathcal{K} , which implies that the system is an input-to-state stability (ISS) system with Δv_1 as the input. By [40], we have

$$|y(t)| \leq C \cdot |x| \leq \sigma_y(|x(0)|, t) + \gamma_y(\|\Delta v_{i-1}\|) \tag{33}$$

where $\sigma_y(|x(0)|, t) = C_M \exp\left(-\psi_1/2\lambda_m\right)t\sqrt{(\lambda_M/\lambda_m)}|x(0)|$ also belongs to \mathcal{KL} and $\gamma_y(\|\Delta v_{i-1}\|) = C_M \sqrt{(\psi_2/\psi_1)}\|\Delta v_{i-1}\|$ is also a function of \mathcal{K} .

Now, we can conclude that system (6) is an IOS system.

Discussion: For the linear sample-based system with disturbance, when the data processing is performed at the sampling point and the feedback gain is updated, a change in the control law or a switch in controllers easily causes the instability of the system. According to [41], when the sample period (or data rate) satisfies the following assumptions, the system maintains stability.

Assumption 1: The sampling period T satisfies

$$\Omega_p := \left| e^{AT} \right|_{\infty} < N. \tag{34}$$

The inequality in (34) can be interpreted as a lower limit on the data rate Ω_p because it needs a sufficiently short sampling time T in relation to N . N has the same bound

as [42, Assumption 3] and a similar bound appearance in [43] for a single model with limited information.

According to the proof of [44, Lemma 1], the following condition holds:

$$\sigma_{pi} \doteq \frac{1}{N} \left\| C A \tilde{C}^{\dagger} \right\| < 1 \tag{35}$$

where $\tilde{C} = \Gamma_i \cdot A^{-i+1}$, and then the controller will possess the convergence property.

In the case of state feedback, (35) becomes $\|A\|/N < 1$. Our algorithm and proof do not require the same N at every sampling time. With different N at every sampling time, represented by N_k , the inequality $\|A\|/N < 1$ can be rewritten as follows: for all f , there exists f' that satisfies $\prod_{l=f}^{f+f'} \|A\|/N_l < 1$. Therefore, any $\tilde{N} > \|A\|$ can be chosen, where \tilde{N} is the geometric average of N and can still satisfy the convergence property of the controller.

For scalar systems where $A = a > 0$, $\|A\| = \exp(aT_s) = \eta_1$, and we can then choose any average $\tilde{N} > |\eta_j|$. For a multidimensional system, when A becomes a real symmetric matrix through diagonalization, we can apply a $1 - D$ quantizer for the quantitative system. For paired conjugate complex eigenvalues, η_j and $\eta_{\bar{j}} = \bar{\eta_j}$, we can choose a rotated 2-D square quantizer with a rotation rate of $\angle \eta_j$. In the above case, the number of quantized regions in each dimension corresponds to the growth rate of $|\eta_j|$.

Therefore, it is fair to say that Assumption 1 does not introduce significant conservatism beyond requiring that the data rate be sufficient to stabilize system (6).

The robustness proof is thus completed. \blacksquare

B. String Stability

The \mathcal{L}_2 string stability of interconnected vehicles takes the influence of external disturbance into account. Due to the “overlapping” topology, Δv_1 appears to be the true disturbance. Consider φ as the external input to the lead vehicle. Then, the assumption is given as follows.

Assumption 2: For any initial values $\Delta h_1(0)$ and $\Delta v_1(0)$, and any $\varphi \in \mathcal{L}_2$, there are two functions ζ_1 and ζ_2 that belong to class \mathcal{K} such that

$$|\Delta v_1|_{\mathcal{L}_2} \leq \zeta_1(|\varphi|_{\mathcal{L}_2}) + \zeta_2(|[\Delta h_1(0), \Delta v_1(0)]^T|). \tag{36}$$

First, for analyzing \mathcal{L}_2 string stability, the following definitions are determined.

Definition 1: The system (6) is \mathcal{L}_2 string stable if, for any initial state $\bar{x}(0) \in \mathbb{R}^{2n+2}$, the functions ζ_3, ζ_4 belong to class \mathcal{K}

$$|\Delta v_1|_{\mathcal{L}_2} \leq \zeta_3(|\varphi|_{\mathcal{L}_2}) + \zeta_4(|\bar{x}(0)|). \tag{37}$$

Then, under Assumption 2 and Definition 1, we obtain the string stability conclusion shown as follows.

Theorem 2: If Assumption 2 holds, the closed-loop system (6) is \mathcal{L}_2 string stable with each of the optimal controllers.

Proof: We divide the proof process into two steps. First, after the above system stability analysis, we can obtain that Δv_i holds the following inequality for any initial state $x(0)$:

$$|\Delta v_i| \leq \phi_1 e^{-at} |x(0)| + \phi_2 \|\Delta v_1\| \tag{38}$$

TABLE II
PARAMETERS FOR CONTROLLER DESIGN AND SIMULINK

Par	Mean	Value	Unit
h^*	Desired headway	30	m
v^*	Desired velocity	25	m/s
v_{\max}	Maximum velocity	30	m/s
h_{stop}	Stop headway	5	m
\tilde{h}_2/\tilde{h}_4	Stop headway of vehicle 2 and 4	5	m
ΔT	Sampling time	0.01	s
τ_2/τ_4	Designed CTH of vehicle 3 and 5	1	s
v_0^1	Initial velocity of the leading vehicle	25	m/s
$v_0^2/v_0^3/v_0^4$	Initial velocity of the other vehicles	20	m/s
h_0	Initial distance	20	m
α_i/β_i	Human parameters	6/0.6	—

where $\phi_1 = \sqrt{(\lambda_M/\lambda_m)}$, $a = (-d_1/2\lambda_m)$, $\phi_2 = \sqrt{(d_2/d_1)}$. Then, we can easily obtain

$$|\phi_1 e^{-at}|_{\mathcal{L}_2} \leq \phi_1 \left(\frac{1}{2a} \right)^{1/2}. \quad (39)$$

From (33) and (39), we obtain

$$\begin{aligned} |\Delta v_i|_{\mathcal{L}_2} &\leq \phi_1 \left(\frac{1}{2a} \right)^{1/2} |x(0)| + \phi_2 |\Delta v_1|_{\mathcal{L}_2} \\ &:= \zeta_5 (|\Delta v_1|_{\mathcal{L}_2}) + \zeta_6 (|x(0)|). \end{aligned} \quad (40)$$

Through the above analysis, we can find that there exist two functions ζ_5 and ζ_6 of class \mathcal{K} that satisfy the inequality in \mathcal{L}_2 space.

Second, by combining Assumption 1, it is easy to obtain (40) by allowing

$$\begin{aligned} \zeta_3 &= \zeta_5 \circ \zeta_1 \\ \zeta_4 &= \zeta_5 \circ \zeta_2 + \zeta_6. \end{aligned}$$

This proof is completed. \blacksquare

According to the small-gain theorem, the platoon is defined as being strictly \mathcal{L}_2 string stable if all subsystems meet the requirement of input and output gain less than 1. This condition may not be satisfied because the platoon includes human-driven vehicles. Therefore, the string stability of the autonomous vehicle is ensured by the proof.

V. SIMULATIONS

To demonstrate the effectiveness of the proposed DDMPC method for hybrid connected vehicles, we perform simulation experiments using MATLAB/Simulink and CarSim. Taking into account the limited communication range and random packet loss in practice [33], and according to our research objectives, we study a platoon of four vehicles, two of which (the first and third vehicles) are driven by humans and have different human parameters. Table II shows the system parameters, whereas throughout the data processing phase, the human parameters α_i and β_i are considered to be unknown for autonomous vehicles. According to [45], the V2V simulation module is built through the TrueTime toolbox to establish the communication topology, which can realize vehicle information transmission. For analysis and processing, historical headway and velocity data acquired during real-time simulation are employed.

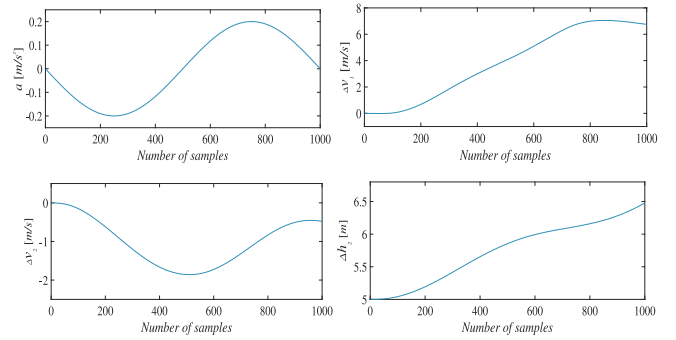


Fig. 4. Input and output data for identification.

The simulation test is divided into the following two parts. First, the exciting input signal is constructed according to the features of the plant, and the velocity fluctuation Δv_1 of the leading vehicle as the measured disturbance is used for identification and predictor construction. Then, another set of signal data is chosen to assess the constructed predictor. Second, the proposed control method is tested by simulation in multiple scenarios to assess the efficacy and superiority of the control law and communication topology. The detailed design process and analysis are presented as follows.

A. Data Identification and Verification Results

The experimental settings and tuning control parameters are described before presenting the simulation. Identification data are collected while traveling on a straight road, fixed expected speed $v^* = 36$ m/s, initial velocity $v_0 = 36$ m/s, and initial spacing $d = 20$ m for the platoon. According to [34] and [35], to minimize the impact of communication delay on system performance and stability, the time headway τ is set to 1. The CarSim model is simulated with a frequency of 1000 Hz. The operation frequency of the simulation is 100 Hz, which is selected based on the platoon control requirements and the analysis of the sampling period on the vehicle control performance in [46]. For verification, the number of vehicles does not affect the recognition accuracy, so the same conclusion can be obtained in a simple way. Here, we take two cars to design the predictor, in which the first vehicle is human-operated and the second vehicle is an autonomous vehicle. To obtain the identification data, the acceleration as the input signal for the autonomous vehicle is designed during the movement.

For the design of the predictor, the parameters to be chosen are the rows and columns of the Hankel matrix constructed based on data, as shown in Table I, where $i = 50$ and $j = 50$, respectively. Following that, in regard to controller design, the prediction horizon $N_p = 5$ and the control horizon $N_u = 5$. Fig. 4 depicts the open-loop data set of the input a , measured disturbance Δv_1 , and output Δv_2 for identification. Another set of signal data is utilized to assess the identification results of the predictor, and the results are depicted in Fig. 5.

According to the verification result, the predictive outputs Δv_2^* and Δh_2^* constructed by the predictor can be accurate in matching the true outputs Δv_2 and Δh_2 of the model.

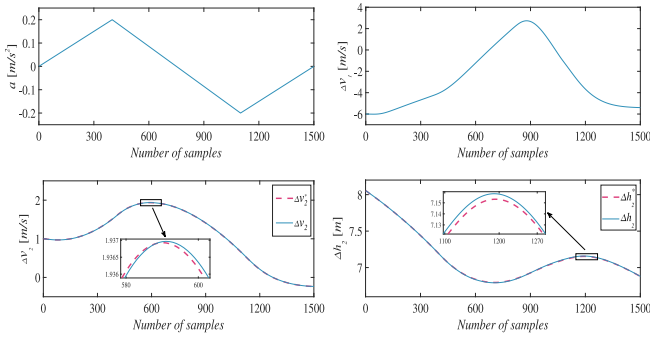


Fig. 5. Input and output data for verification and identification results.

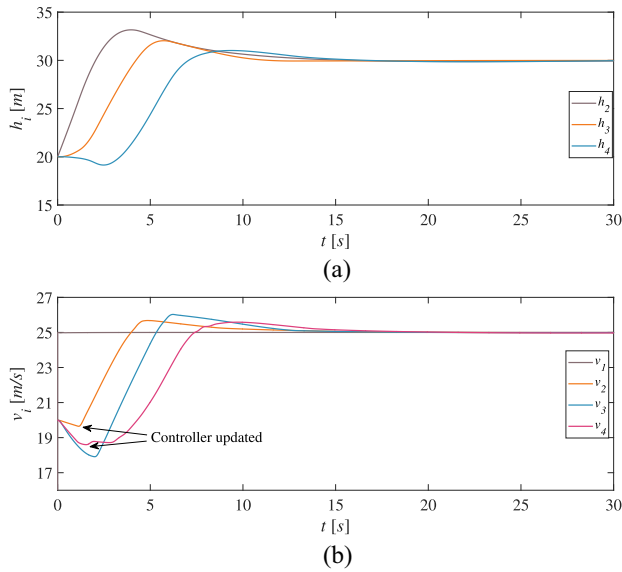


Fig. 6. Spacing and speed profiles of vehicles controlled by DMPC. (a) Spacing of vehicles controlled by DMPC. (b) Speed of vehicles controlled by the DMPC.

B. Simulation Condition Design and Simulation Result

This section presents five experiments to verify the performance of DDMPC. In the first simulation, the leader and the third vehicle are human driven, and the other two are autonomous. In the data collection phase, the automatic driving vehicle is driven according to the preset controller in the data acquisition and processing phase. Subsequently, it switches to the data-driven controller.

The first simulation results for the trajectories of the headway and velocity of vehicles when the desired speed remains constant and the leading vehicle is driving at the desired speed are shown in Fig. 6. The simulation plots clearly indicate that all the vehicles can maintain the same headway after $t = 15$ s and track the desired speed at the same time, which implies that the control system is asymptotically stable. Note that the space fluctuation decreases gradually along the platoon and that the velocity fluctuation of the autonomous vehicle (e.g., vehicle 4) has a smaller amplitude than that of the other vehicles. The results verify the string stability of the autonomous vehicles in the platoon.

Similar to the first condition in Table II, the initial velocity and initial space of adjacent vehicles are changed in this

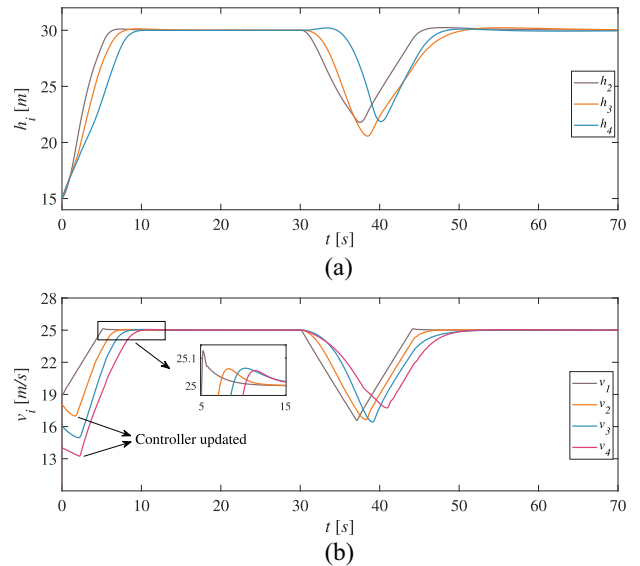


Fig. 7. Spacing and speed profiles when the velocity of the leader suddenly changes. (a) Spacing of vehicles at sudden speed change. (b) Speed of vehicles at sudden speed change.

condition. To simulate expected speed changes due to an emergency during driving and verify the performance of DDMPC in the face of disturbance, at $t = 30$ s, we set $v^* = 16$ m/s, and after $t = 37$ s, we return v^* to 25 m/s. The regulation process of the spacing and speed of vehicles is shown in Fig. 7. The speed amplitude of vehicle 2 is less than that of the leader, and for vehicle 4, the amplitude is smaller than that of the other vehicles. The same results can be obtained for the fluctuation of spacing. On the other hand, the velocity fluctuation of human-operated vehicle 3 may be greater than that of the first two vehicles. The simulation results demonstrate that the autonomous vehicle can still maintain string stability while converging to the desired headway and velocity. We can therefore conclude that the designed feed-forward controller has strong robustness against the measured disturbance.

Comparison With the Model-Based Control Method: As a classical model-based method, MPC is widely employed in the field of automatic control. Therefore, we compare it with DDMPC. The nominal value $\tilde{\alpha} = 1$, $\tilde{\beta} = 0.2$ is used in the construction of the MPC controller. It is apparent from the findings shown in Fig. 8 that the headway is only $h_5 = 12.4$ m when the speed of the autonomous vehicle is $v_5 = 19$ m/s at $t = 3$ s, which may affect the safety of the platoon. The reason is that the model-based approach presupposes that all driver parameters are known precisely. Therefore, for the nonoptimal controller designed by the model-based method with unknown parameters, safety is a concern. For the fluctuation in spacing and speed, the peak values are reported in Table III. The peak is defined as $\Phi_p := \max_{0 \leq t' \leq t} \Phi$, where Φ denotes speed and spacing. The average reduction (AR) compared to other cases is defined as

$$AR := \frac{(\Phi_{pd} - \Phi_p^*) - (\Phi_{po} - \Phi_p^*)}{\Phi_{po} - \Phi_p^*} \times 100\%$$

TABLE III
SIMULATION RESULT DATA IN DIFFERENT SCENARIOS

Control type	Speed peak (m/s)		Space peak (m)	
	v_2	v_4	h_2	h_4
DMPC	25.6797	25.5847	33.1627	31.0206
MPC	25.7927	25.7017	33.2283	32.8696
ACC	25.6797	26.7168	33.1627	32.8885
Average	Compare to MPC	14.26%	16.67%	2.03%
Reduction	Compare to ACC	0%	65.94%	0
				64.67%

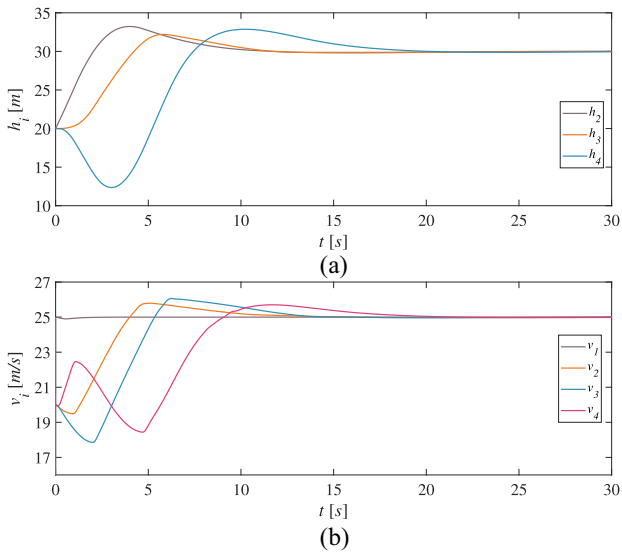


Fig. 8. Spacing and speed profiles of vehicles controlled by MPC. (a) Spacing in ACC vehicles. (b) Speed in ACC vehicles.

where Φ_{pd} and Φ_{po} denote the peak of DMPC and other cases, respectively, and Φ_p^* denote the desired speed and spacing. The autonomous vehicles controlled by DMPC reduce the speed peak value by 14.26% and 16.67% from the model-based method. At the same time, the decrease in the spacing peak increases from 2.03% to 64.61% along the platoon. This indicates that the approach presented in this article has a significantly better capability to maintain string stability for autonomous vehicles.

Comparison With ACC: The autonomous vehicles are equipped with ACC equipment, and DMPC is used to design the controller. Fig. 9 depicts the control results in this simulation. A similar analysis is carried out under the above conditions; the connected vehicles are not string stable. The evaluation results are summarized in Table III. Overall, ACC leads to 65.94% speed amplification and 64.67% spacing amplification. The main reason is that vehicles equipped with ACC can receive information from the adjacent preceding vehicle only and cannot respond to changes in the movement of other vehicles. In comparison, vehicles that can obtain more information about the other vehicles through V2V communication will potentially improve the robustness and string stability of connected vehicles.

Slowdowns: To illustrate that the DDMPC method is adaptable to a variety of different scenarios, the control effect of the platoon is evaluated in the slowdown scenario with the same

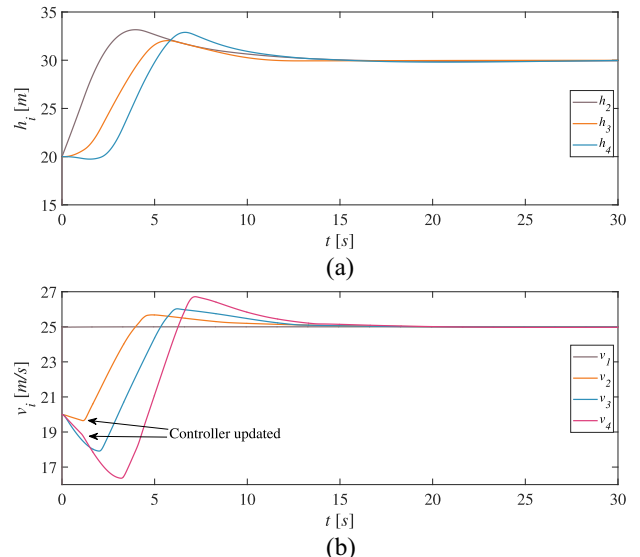


Fig. 9. Spacing and speed profiles of ACC vehicles controlled by DMPC. (a) Spacing in ACC vehicles. (b) Speed in ACC vehicles.

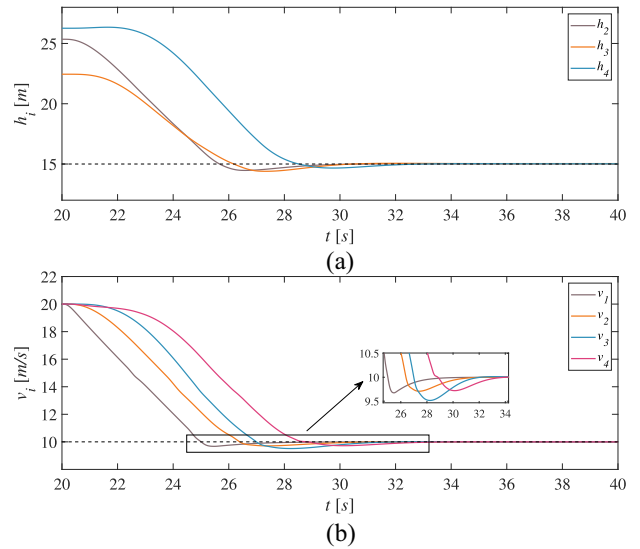


Fig. 10. Spacing and speed profiles of connected vehicles when the leader slows down. (a) Spacing when the leader slows down. (b) Speed when the leader slows down.

initial velocity and different initial spacing. In this condition, $v^* = 10$ m/s, and $v_0 = 20$ m/s. The results are demonstrated in Fig. 10. A similar conclusion can be drawn that the CAV controlled by a distributed data-driven predictive controller can ensure string stability with no steady-state tracking error while completing the CTH strategy.

Platoon Expansion: Finally, we studied the scalability of the proposed method by increasing the number of vehicles in the platoon. The new multivehicle system consists of seven vehicles, of which 1.3.5 vehicles are human-driven and the others are autonomous vehicles. In this simulation, the leading vehicle travels at a varying speed of 0–35 m/s and finally remains constant. The initial spacing of all vehicles in the platoon is 30 m. Fig. 11(a) and (b) shows the control results of speed and spacing. The CAVs caused no speed overshoot for frequent speed changes. This means that human-driven

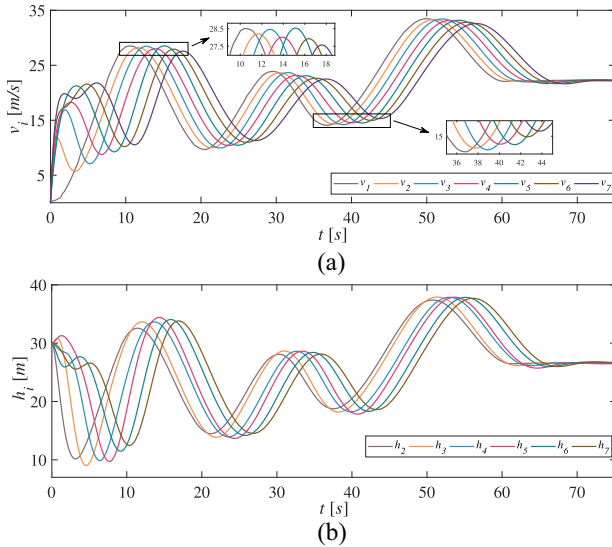


Fig. 11. Spacing and speed profiles of connected vehicles in platoon expansion simulation. (a) Spacing of vehicles in the simulation. (b) Speed of vehicles in the simulation.



Fig. 12. Physical picture of the driver-in-the-loop platform.

speed oscillation is always mitigated by autonomous vehicles; thus, robustness and string stability are guaranteed.

For the platoon with more followers, it is only necessary to collect more vehicle motion data to construct a new subspace predictor, and the proof of L_2 string stability also ensures that the DDMPC method we proposed is not affected by the number of vehicles.

VI. EXPERIMENTS

This section discusses bench experiments to evaluate the performance of the proposed method.

A. Bench Experiment Devices

To perform the experiments, a driver-in-the-loop test platform is built to conduct experiments in real driving scenarios. The relevant devices include the visualization module, brake pedal, accelerator pedal and steering wheel. The structure diagram and experimental equipment are shown in Figs. 12 and 13, respectively. We communicate with the PC host via the controller area network (CAN) bus and send operation commands, such as braking and acceleration to the

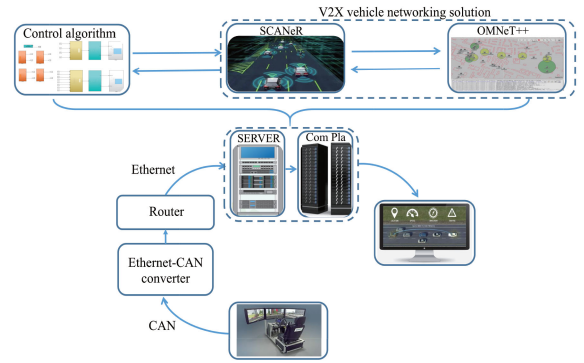


Fig. 13. Structure diagram of driver-in-the-loop platform.

controlled simulated vehicle, which are then displayed in the visualization module.

The dynamics software is implemented in SCANeR and MATLAB/Simulink, whose programs run on the server and intelligent connected vehicle (ICV) computing platform. The controller is designed in Simulink and finally input into SCANeR to complete the control command. In the experiment, we use the objective modular network testbed in C++ (OMNeT++) to realize wireless communication between vehicles in platoons by sending beacons, in which the medium access control (MAC) and physical layers are based on the IEEE 802.11p standard protocol adopted for V2V.

B. Experimental Design and Results

According to the previous analysis, we have the same choice here for the experimental design for the platoon composed of four vehicles. Among them, autonomous vehicles are controlled by the DDMPC approach in this article. For the human-driven car, we choose two drivers to operate the first and third vehicles according to relevant cruise instructions. To simulate the real driving behavior, the driving speed of the head driver is time-varying. The sampling frequency of the SCANeR is set to 100 Hz. Before the experiment, the vehicle's motion state was collected, and the data collection time was 10 s. First, the vehicle's motion state is collected. The data collection time is 10 s. After the data collection, the controller design is completed offline. Then, the controller is implemented in cooperative control, and the results are shown in Figs. 14 and 15. We divide the entire driving process into two processes: acceleration and deceleration. The acceleration process is divided into three stages, and the deceleration process is divided into two stages. The corresponding data analysis is provided in Tables IV and V.

Fig. 14 shows the regulation process of the hybrid platoon controlled by DDMPC in the presence of external disturbance. It can be seen from the partial magnified pictures of speed that because of the reaction time of the driver, human-driven vehicles have a tendency to amplify speed variations in reaction to sudden variations in the speed of the preceding vehicle. However, the speed fluctuations for the following autonomous vehicles are decreased, and the reduction of the latter autonomous vehicle is less than that of the other autonomous vehicles in front, indicating that the autonomous

TABLE IV
SUMMARY OF EXPERIMENTAL DATA

		Speed peak (m/s)				Fluctuation reduction	Average reduction compare to MPC
		v_1	v_2	v_3	v_4		
Acceleration	Stage 1	25.4555	25.2205	25.9124	24.8054	57.88%	18.57%
	Stage 2	24.7253	24.5119	24.8974	24.1162	41.17%	12.89%
	Stage 3	29.9625	29.8078	29.8532	29.1892	77.01%	27.49%
Braking	Stage 1	15.3831	15.6884	15.4489	16.4071	61.78%	17.18%
	Stage 2	19.7013	19.9425	19.6767	20.2877	46.17%	14.34%

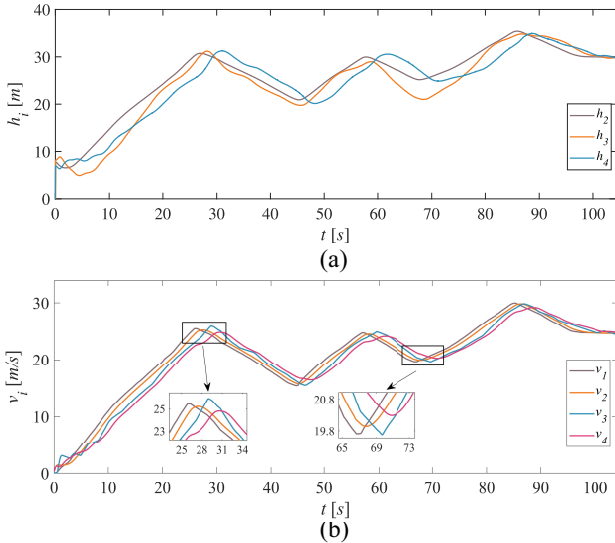


Fig. 14. Spacing and speed profiles of connected vehicles when the driver is in the loop. (a) Spacing when the driver in the loop. (b) Speed when the driver in the loop.

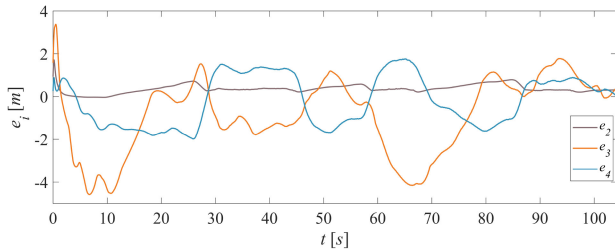


Fig. 15. Spacing error of connected vehicles when the driver is in the loop.

vehicles are string stable. Considering that there are human-driven vehicles in the platoon and the driving characteristics of the driver are unknown, the system has dynamic uncertainties, which makes it impossible to adopt the mechanism model. The DDMPC proposed in this article completes the construction of the multivehicle system by collecting data, and the autonomous vehicle achieves the control target while ensuring string stability, which not only proves the feasibility of the method but also verifies the theoretical analysis in Section IV.

To quantify the system performance, Tables IV and V provide the data results related to speed and spacing error. It can be seen from the data in Table IV that the speed fluctuation reduction percentages of the three acceleration stages are 57.88%, 41.17%, and 77.01% and reduced by 61.78% and

TABLE V
SUMMARY OF EXPERIMENTAL DATA

	e_2	e_3	e_4	Average reduction
Spacing error RMS(m)	0.4246	1.9678	1.1818	39.9431%

46.17% in the deceleration phase, which indicates that the autonomous vehicles can mitigate the speed oscillation at each stage. The results are consistent with the simulation analysis in Section V. In addition, the AR in spacing error, expressed as the root mean square (RMS), is 39.94%, which means that autonomous vehicles controlled by DDMPC can also suppress the fluctuation of the spacing error. Therefore, Tables IV and V fully confirm the effectiveness of the proposed strategy.

Fig. 16 shows the speed results of the bench experiment under different control and cruise modes for comparative analysis. Fig. 16(a) shows the control performance under the ACC model. In this experiment, the autonomous vehicle can receive information only from the previous vehicle for learning the optimal controller. It can be seen from the speed fluctuations in the time intervals 25–34 s and 65–71 s that braking and accelerating characteristics are slowly transmitted to the tail of the platoon. Compared with the communication topology used in this article, the control of this mode does not take into account the speed variation of the lead vehicle, and the selection of the time gap is different from CAVs. Thus, the system fails to maintain string stability. Fig. 16(b) is the second comparison, which uses the MPC method with nominal parameters to control the hybrid platoon. We can see from the results that it is not an optimal controller. Although the nonoptimal controller can maintain string stability, its ability to suppress the speed fluctuation of autonomous vehicles is weaker. According to the data summary in Table IV, compared with MPC, the peak AR of DDMPC is 18.57%, 12.89%, 27.49%, 17.18%, and 14.34% for the five driving stages, which means that the DDMPC method can improve the efficiency of suppressing speed fluctuations, potentially increasing the robustness of connected vehicles.

In summary, combined with the experimental results in Figs. 14–16 and the data analysis in Tables IV and V, for a hybrid platoon system with unknown dynamics, under the DDMPC collaboration strategy proposed in this article, CAVs have the ability to efficiently attenuate velocity oscillation. This ensures string stability and improves the control performance. Specifically, this strategy uses the V2V communication topology to collect data to establish a subspace

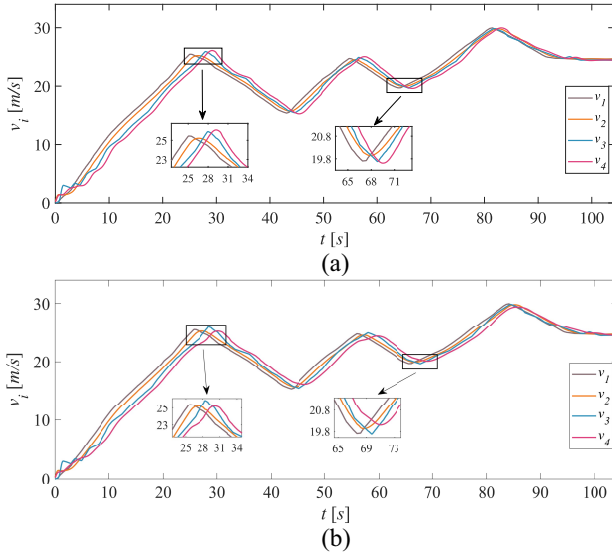


Fig. 16. Speed profiles in bench experiments with different controls. (a) Speed profiles of ACC vehicles controlled by DMPC. (b) Speed profiles of CCC vehicles controlled by MPC.

predictor. This model is different from the mechanism-based model in the traditional MPC and can more accurately approximate the system characteristics with uncertain dynamics. The optimal controller, including feedforward compensation designed based on this subspace model, has better capabilities for vehicle control and system stability. In addition, this scheme outperforms the other two schemes in Fig. 16, further verifying its advantage in maintaining string stability.

VII. CONCLUSION

In this article, we developed a DDMPC approach for a hybrid platoon system composed of human-driven and autonomous vehicles in the presence of disturbances and unknown system parameters. The predictor and controller were constructed by combining the input and output information from the connected vehicles directly. System stability and string stability were taken into account within the proposed method: robustness of the interconnected platooning system was examined by using sampled-data systems theory and input-to-output stability (IOS) theory comprehensively, and \mathcal{L}_2 -norm string stability was guaranteed by considering the disturbance attenuation along the platoon. This study obtained rigorous mathematical proofs for stability using the nonlinear systems theory.

To verify the effectiveness and superiority of this method, simulations on CarSim and bench experiments were carried out. The results confirmed the accuracy of the mathematical analysis and proof of the designed controller. In addition, according to the results, the DDMPC scheme can not only meet the control objectives of ensuring the desired velocity and headway but also exhibits improved performance in string stability compared with model-based methods and ACC.

Future research is needed in light of the findings of this study. Our future work will focus on the modeling mechanism and performance analysis under the combined effect of data

delay and packet loss and ensure system stability through the data-driven approach. The mathematical analysis in this article lays critical groundwork for these possible extensions.

REFERENCES

- [1] S. Heo, W. Yoo, H. Jang, and J.-M. Chung, "H-V2X mode 4 adaptive semi-persistent scheduling control for cooperative Internet of Vehicles," *IEEE Internet. Things.*, vol. 8, no. 13, pp. 10678–10692, Jul. 2021.
- [2] L. Tao, Y. Watanabe, Y. Li, S. Yamada, and H. Takada, "Collision risk assessment service for connected vehicles: Leveraging vehicular state and motion uncertainties," *IEEE Internet. Things.*, vol. 8, no. 14, pp. 11548–11560, Jul. 2021.
- [3] Y. Chen, C. Lu, and W. Chu, "A cooperative driving strategy based on velocity prediction for connected vehicles with robust path-following control," *IEEE Internet Things J.*, vol. 7, no. 5, pp. 3822–3832, May 2020.
- [4] Q. Zhang, H. Zhong, J. Cui, L. Ren, and W. Shi, "AC4AV: A flexible and dynamic access control framework for connected and autonomous vehicles," *IEEE Internet Things J.*, vol. 8, no. 3, pp. 1946–1958, Feb. 2021.
- [5] G. Marsden, M. McDonald, and M. Brackstone, "Towards an understanding of adaptive cruise control," *Transp. Res. C, Emerg. Technol.*, vol. 9, no. 1, pp. 33–51, Feb. 2001.
- [6] C. Campolo, A. Molinaro, A. Iera, and F. Menichella, "5G network slicing for vehicle-to-everything services," *IEEE Wireless Commun.*, vol. 24, no. 6, pp. 38–45, Dec. 2017.
- [7] F. Zhang, M. M. Wang, X. Bao, and W. Liu, "Centralized resource allocation and distributed power control for NOMA-integrated NR V2X," *IEEE Internet. Things J.*, vol. 8, no. 22, pp. 16522–16534, Nov. 2021.
- [8] S. Darbha, S. Kondu, and P. R. Pagilla, "Benefits of V2V communication for autonomous and connected vehicles," *IEEE Trans. Intell. Transp. Syst.*, vol. 20, no. 5, pp. 1954–1963, May 2019.
- [9] H. Liu, X. D. Kan, S. E. Shladover, X.-Y. Lu, and R. E. Ferlisi, "Modeling impacts of cooperative adaptive cruise control on mixed traffic flow in multi-lane freeway facilities," *Transp. Res. C, Emerg. Technol.*, vol. 95, pp. 261–279, 2018.
- [10] Y. Bian, Y. Zheng, W. Ren, S. E. Li, J. Wang, and K. Li, "Reducing time headway for platooning of connected vehicles via V2V communication," *Transp. Res. C, Emerg. Technol.*, vol. 102, pp. 87–105, May 2019.
- [11] S. Calvert *et al.*, "Traffic flow of connected and automated vehicles: Challenges and opportunities," in *Road Vehicle Automation*, vol. 4. Cham, Switzerland: Springer, 2018, pp. 235–245.
- [12] W.-X. Zhu and H. M. Zhang, "Analysis of mixed traffic flow with human-driving and autonomous cars based on car-following model," *Physica A Stat. Mech. Appl.*, vol. 496, pp. 274–285, Apr. 2018.
- [13] D. He, Y. Shi, H. Li, and H. Du, "Multiobjective predictive cruise control for connected vehicle systems on urban conditions with InPA-SQP," *Optim. Control Appl. Methods*, vol. 40, no. 3, pp. 479–498, 2019.
- [14] I. G. Jin and G. Orosz, "Optimal control of connected vehicle systems with communication delay and driver reaction time," *IEEE Trans. Intell. Transp. Syst.*, vol. 18, no. 8, pp. 2056–2070, Aug. 2017.
- [15] L. D. Berkovitz, *Optimal Control Theory*, vol. 12. New York, NY, USA: Springer, 2013.
- [16] D. Zhao, Z. Xia, and Q. Zhang, "Model-free optimal control based intelligent cruise control with hardware-in-the-loop demonstration [research frontier]," *IEEE Comput. Intell. Mag.*, vol. 12, no. 2, pp. 56–69, May 2017.
- [17] Y. Zhu, D. Zhao, and Z. Zhong, "Adaptive optimal control of heterogeneous cacc system with uncertain dynamics," *IEEE Trans. Control Syst. Technol.*, vol. 27, no. 4, pp. 1772–1779, Jul. 2019.
- [18] H. Guo, J. Liu, Q. Dai, H. Chen, Y. Wang, and W. Zhao, "A distributed adaptive triple-step nonlinear control for a connected automated vehicle platoon with dynamic uncertainty," *IEEE Internet Things J.*, vol. 7, no. 5, pp. 3861–3871, May 2020.
- [19] W. Gao, Z.-P. Jiang, and K. Ozbay, "Data-driven adaptive optimal control of connected vehicles," *IEEE Trans. Intell. Transp. Syst.*, vol. 18, no. 5, pp. 1122–1133, May 2017.
- [20] A. Haber and M. Verhaegen, "Subspace identification of large-scale interconnected systems," *IEEE Trans. Autom. Control*, vol. 59, no. 10, pp. 2754–2759, Oct. 2014.
- [21] W. Favoreel, B. De Moor, and M. Gevers, "SPC: Subspace predictive control," *IFAC Proc. Vol.*, vol. 32, no. 2, pp. 4004–4009, 1999.
- [22] E. F. Camacho and C. B. Alba, *Model Predictive Control*. London, U.K.: Springer, 2013.

- [23] R. Kadali, B. Huang, and A. Rossiter, "A data driven subspace approach to predictive controller design," *Control Eng. Pract.*, vol. 11, no. 3, pp. 261–278, 2003.
- [24] G. H. Golub and C. F. Van Loan, *Matrix Computations*, vol. 3. Baltimore, MD, USA: John Hopkins Univ. Press, 2013.
- [25] D. Swaroop and J. K. Hedrick, "String stability of interconnected systems," *IEEE Trans. Autom. Control*, vol. 41, no. 3, pp. 349–357, Mar. 1996.
- [26] F. Ma *et al.*, "Eco-driving-based cooperative adaptive cruise control of connected vehicles platoon at signalized intersections," *Transp. Res. D, Transp. Environ.*, vol. 92, Mar. 2021, Art. no. 102746.
- [27] Y. Li, C. Tang, K. Li, X. He, S. Peeta, and Y. Wang, "Consensus-based cooperative control for multi-platoon under the connected vehicles environment," *IEEE Trans. Intell. Transp. Syst.*, vol. 20, no. 6, pp. 2220–2229, Jun. 2019.
- [28] J. Ploeg, D. P. Shukla, N. van de Wouw, and H. Nijmeijer, "Controller synthesis for string stability of vehicle platoons," *IEEE Trans. Intell. Transp. Syst.*, vol. 15, no. 2, pp. 854–865, Apr. 2014.
- [29] G. Naus, R. P. A. Vugts, J. Ploeg, M. J. G. van de Molengraft, and M. Steinbuch, "String-stable CACC design and experimental validation: A frequency-domain approach," *IEEE Trans. Veh. Technol.*, vol. 59, no. 9, pp. 4268–4279, Nov. 2010.
- [30] J. Ploeg, N. Van De Wouw, and H. Nijmeijer, "LP string stability of cascaded systems: Application to vehicle platooning," *IEEE Trans. Control Syst. Technol.*, vol. 22, no. 2, pp. 786–793, Mar. 2014.
- [31] B. Picasso, D. Desiderio, and R. Scattolini, "Robust stability analysis of nonlinear discrete-time systems with application to MPC," *IEEE Trans. Autom. Control*, vol. 57, no. 1, pp. 185–191, Jan. 2012.
- [32] M. A. Müller, D. Angeli, and F. Allgöwer, "On necessity and robustness of dissipativity in economic model predictive control," *IEEE Trans. Autom. Control*, vol. 60, no. 6, pp. 1671–1676, Jun. 2015.
- [33] C. Zhao, L. Cai, and P. Cheng, "Stability analysis of vehicle platooning with limited communication range and random packet losses," *IEEE Internet Things J.*, vol. 8, no. 1, pp. 262–277, Jan. 2021.
- [34] X. Liu, A. Goldsmith, S. S. Mahal, and J. K. Hedrick, "Effects of communication delay on string stability in vehicle platoons," in *Proc. IEEE Conf. Intell. Transp. Syst.*, 2001, pp. 625–630.
- [35] J. Ploeg, N. van de Wouw, and H. Nijmeijer, "Fault tolerance of cooperative vehicle platoons subject to communication delay," *IFAC-PapersOnLine*, vol. 48, no. 12, pp. 352–357, 2015.
- [36] K. Li, Y. Bian, S. E. Li, B. Xu, and J. Wang, "Distributed model predictive control of multi-vehicle systems with switching communication topologies," *Transp. Res. C, Emerg. Technol.*, vol. 118, Sep. 2020, Art. no. 102717.
- [37] Y. Zheng, S. E. Li, K. Li, F. Borrelli, and J. K. Hedrick, "Distributed model predictive control for heterogeneous vehicle platoons under unidirectional topologies," *IEEE Trans. Control Syst. Technol.*, vol. 25, no. 3, pp. 899–910, May 2017.
- [38] W. B. Dunbar and D. S. Caveney, "Distributed receding horizon control of vehicle platoons: Stability and string stability," *IEEE Trans. Autom. Control*, vol. 57, no. 3, pp. 620–633, Mar. 2012.
- [39] J. P. Hespanha, *Linear Systems Theory*. Princeton, NJ, USA: Princeton Univ. Press, 2018.
- [40] E. D. Sontag, "Input to state stability: Basic concepts and results," in *Nonlinear and Optimal Control Theory*, P. Nistri and G. Stefani, Eds. Berlin, Germany: Springer, 2008, pp. 163–220.
- [41] G. Yang and D. Liberzon, "Feedback stabilization of switched linear systems with unknown disturbances under data-rate constraints," *IEEE Trans. Autom. Control*, vol. 63, no. 7, pp. 2107–2122, Jul. 2018.
- [42] D. Liberzon, "Finite data-rate feedback stabilization of switched and hybrid linear systems," *Automatica*, vol. 50, no. 2, pp. 409–420, 2014.
- [43] D. Liberzon, "On stabilization of linear systems with limited information," *IEEE Trans. Autom. Control*, vol. 48, no. 2, pp. 304–307, Feb. 2003.
- [44] Y. Sharon and D. Liberzon, "Input to state stabilizing controller for systems with coarse quantization," *IEEE Trans. Autom. Control*, vol. 57, no. 4, pp. 830–844, Apr. 2012.
- [45] A. Garcia-Santiago, J. Castaneda-Camacho, J. F. Guerrero-Castellanos, G. Mino-Aguilar, and V. Y. Ponce-Hinestrosa, "Simulation platform for a VANET using the truetime toolbox: Further result toward cyber-physical vehicle systems," in *Proc. IEEE Veh. Technol. Conf.*, 2018, pp. 1–5.
- [46] A. Ibrahim, D. Goswami, H. Li, I. M. Soroa, and T. Basten, "Multi-layer multi-rate model predictive control for vehicle platooning under IEEE 802.11p," *Transp. Res. C, Emerg. Technol.*, vol. 124, Mar. 2021, Art. no. 102905.



Jingzheng Guo received the M.S. degree in mechanical engineering from Northeastern University, Shenyang, China, in 2019. He is currently pursuing the Ph.D. degree with the Department of Control Theory and Control Engineering, Jilin University, Changchun, China.

His current research interests include the connected and automated vehicles and intelligent transportation system.



Hongyan Guo (Member, IEEE) received the Ph.D. degree from Jilin University, Changchun, China, in 2010.

She joined Jilin University in 2011, where she became an Associate Professor in 2014, and has been a Professor since 2018. She was a Visiting Scholar with Cranfield University, Cranfield, Bedford, U.K., in 2017. Since 2020, she has been a Deputy Director of State Key Laboratory of Automotive Simulation and Control and became the Tang Aoqing Professor with Jilin University in 2020. Her current research

interests include stability control, path planning, and decision making of intelligent vehicles.



Jun Liu received the Ph.D. degree in automation from Jilin University, Changchun, China, in 2020.

He is currently working with the College of Automotive Engineering, Jilin University. His current research interests include vehicle stability control autonomous driving and driver-automation cooperative systems.



Dongpu Cao (Member, IEEE) received the Ph.D. degree from Concordia University, Montreal, QC, Canada, in 2008.

He is currently an Associate Professor and the Director of the Waterloo Cognitive Autonomous Driving (CogDrive) Laboratory, University of Waterloo, Waterloo, ON, Canada. He is the Canada Research Chair in driver cognition and automated driving. He has contributed more than 200 papers and three books. His current research interests include driver cognition, automated driving, and cognitive autonomous driving.

Dr. Cao received the SAE Arch T. Colwell Merit Award in 2012, the IEEE VTS 2020 Best Vehicular Electronics Paper Award, and the three best paper awards from the ASME and IEEE conferences. He serves as the Deputy Editor-in-Chief for *IET Intelligent Transport Systems* and an Associate Editor for *IEEE TRANSACTIONS ON VEHICULAR TECHNOLOGY*, *IEEE TRANSACTIONS ON INTELLIGENT TRANSPORTATION SYSTEMS*, *IEEE/ASME TRANSACTIONS ON MECHATRONICS*, *IEEE TRANSACTIONS ON INDUSTRIAL ELECTRONICS*, *IEEE/CAA JOURNAL OF AUTOMATICA SINICA*, *IEEE TRANSACTIONS ON COMPUTATIONAL SOCIAL SYSTEMS*, and *Journal of Dynamic Systems, Measurement and Control* (ASME). He was a Guest Editor of *Vehicle System Dynamics*, *IEEE TRANSACTIONS ON SYSTEMS, MAN, AND CYBERNETICS-PART A: SYSTEMS*, and *IEEE INTERNET OF THINGS JOURNAL*. He serves on the SAE Vehicle Dynamics Standards Committee and acts as the Co-Chair for IEEE ITSS Technical Committee on Cooperative Driving. He is an IEEE VTS Distinguished Lecturer.



Hong Chen (Senior Member, IEEE) received the Ph.D. degree in system dynamics and control engineering from the University of Stuttgart, Stuttgart, Germany, in 1997.

She joined the Jilin University of Technology, Changchun, China, in 1986, where she became an Associate Professor in 1998 and has been a Professor since 1999. She joined Tongji University, Shanghai, China, in 2019. Her current research interests include model predictive control, optimal and robust control, and applications in process engineering and mechatronic systems.